

Methodologies and Techniques for Detecting Extraterrestrial (Microbial) Life

Terahertz Circular Dichroism Spectroscopy: A Potential Approach to the *In Situ* Detection of Life's Metabolic and Genetic Machinery

JING XU,¹ GERALD J. RAMIAN,¹ JHENNY F. GALAN,² PAVLOS G. SAVVIDIS,¹
ANTHONY MICHAEL SCOPATZ,¹ ROBERT R. BIRGE,² S. JAMES ALLEN,¹
and KEVIN W. PLAXCO³

ABSTRACT

We propose a terahertz (far-infrared) circular dichroism-based life-detection technology that may provide a universal and unequivocal spectroscopic signature of living systems regardless of their genesis. We argue that, irrespective of the specifics of their chemistry, all life forms will employ well-structured, chiral, stereochemically pure macromolecules (>500 atoms) as the catalysts with which they perform their metabolic and replicative functions. We also argue that nearly all such macromolecules will absorb strongly at terahertz frequencies and exhibit significant circular dichroism, and that this circular dichroism unambiguously distinguishes biological from abiological materials. Lastly, we describe several approaches to the fabrication of a terahertz circular dichroism spectrometer and provide preliminary experimental indications of their feasibility. Because terahertz circular dichroism signals arise from the molecular machinery necessary to carry out life's metabolic and genetic processes, this life-detection method differs fundamentally from more well-established approaches based on the detection of isotopic fractionation, "signature" carbon compounds, disequilibria, or other by-products of metabolism. Moreover, terahertz circular dichroism spectroscopy detects this machinery in a manner that makes few, if any, assumptions as to its chemical nature or the processes that it performs. **Key Words:** Far-infrared—Submillimeter—Spectroscopy—Biopolymers—Proteins—DNA—Terahertz—Circular dichroism. *Astrobiology* 3, xxx-xxx.

INTRODUCTION

THE GROWTH OF ASTROBIOLOGY and the rapidly increasing pace of planetary exploration have

fostered significant interest in new methods for the detection of life in extraterrestrial settings such as Mars, Europa, or Titan (e.g., McKay, 1998; National Research Council, 2002). The majority of

Departments of ¹Physics and ³Chemistry and Biochemistry, University of California, Santa Barbara, Santa Barbara, California.

²Department of Chemistry, The University of Connecticut, Storrs, Connecticut.

these technologies focus on the detection of characteristic patterns of organic or inorganic materials (e.g., McKay *et al.*, 1996; Thomas-Keprta *et al.*, 2000), the presence of distinctive isotopic fractionations (e.g., Greenwood *et al.*, 1997; Mojzsis and Arrhenius, 1998), or the observation of significant chemical disequilibria (e.g., Sagan *et al.*, 1993). While each of these approaches is a powerful tool in the quest to detect non-terrestrial life, they all suffer, at least to some extent, from a terrestrial bias. For example, on Earth, polycyclic aromatic hydrocarbons (PAHs) are invariably associated with highly altered fossils (e.g., fossil fuels and their combustion products) and thus are relatively unambiguous signatures of life. Abiological production of PAHs, however, has been suggested for non-terrestrial settings (Zolotov and Shock, 1999), and PAHs are common in the interstellar medium (Henning and Schnaiter, 1998), thus clouding, for example, the suggestion that the PAHs in the Martian meteorite ALH84001 meteorite are biogenic (McKay *et al.*, 1996). Similarly, non-biological isotopic fractionation has been observed (Anbar *et al.*, 2000) that could masquerade as a life signature. Lastly, it is widely held that inorganic chemical disequilibria led to a false detection event when, by analogy to terrestrial life (Klein, 1974), water and simple organic “food” were provided to putative Mars organisms in the Viking experiments (Klein, 1992). We may thus conclude that most contemporary life-detection approaches are complicated by the need to interpret their outcomes in terms of expectations based on the metabolic processes and products of terrestrial references.

We propose here terahertz (far-infrared) circular dichroism (TCD) spectroscopy as perhaps the first of a fundamentally different, and thus complementary, class of life-detection methods. This new approach focuses not on the metabolism or metabolic by-products of life but instead on the *molecular machinery necessary to carry out life processes*. The TCD life-detection approach is based on the argument that stereochemically pure, chiral macromolecules are a universal and unambiguous signature of chemical life (Fig. 1), and that essentially all such macromolecules will exhibit circular dichroism (CD) over a broad range of the terahertz spectrum. We thus believe that TCD will detect the molecular machinery of life in a manner that makes few assumptions as to the chemical nature of this machinery or the processes that it performs.

APPROACH

It is widely appreciated that all macromolecules with ionic or polar constituents absorb strongly across the terahertz part of the spectrum (e.g., Markelz *et al.*, 2000; Globus *et al.*, 2002; Woolard *et al.*, 2002). We have performed simulation studies suggesting that for most, if not all, chiral macromolecules this absorbance will be accompanied by relatively strong CD. We have also designed and are currently building several CD spectrometers operating at terahertz frequencies.

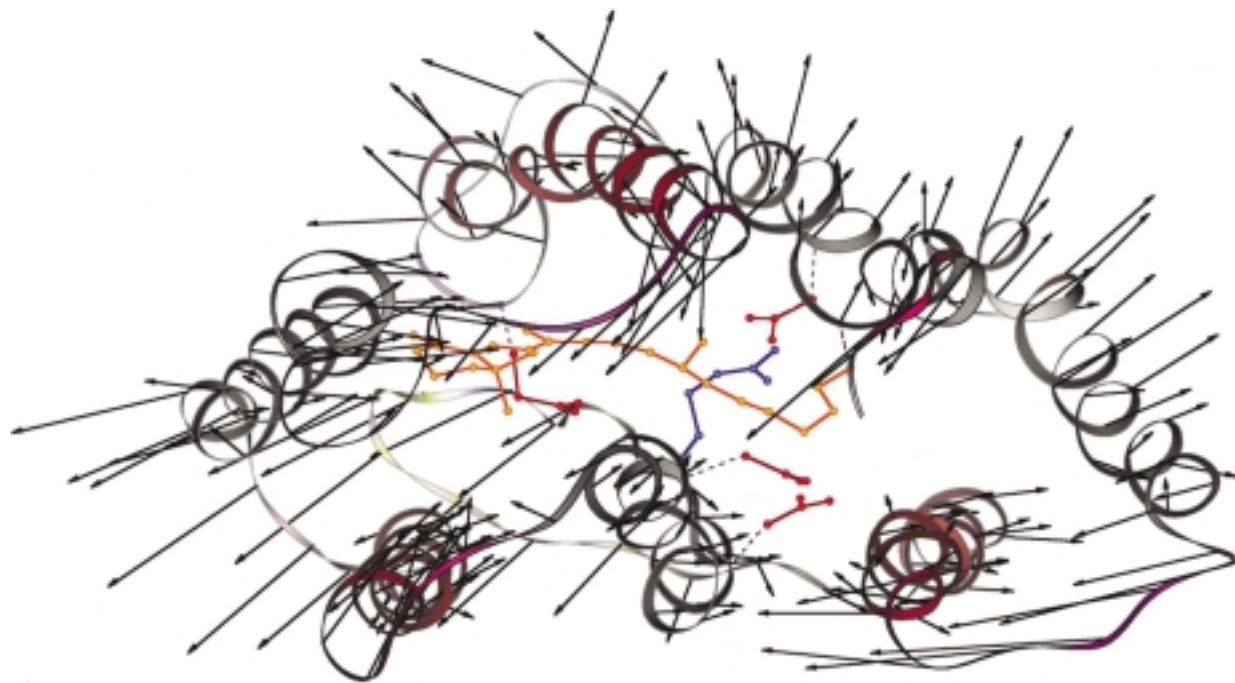
Simulated TCD spectra

While *ab initio* methods have been used to successfully calculate the CD spectra of small molecules, the direct calculation of CD features arising from the collective vibrational modes of macromolecules are computationally intractable. In an effort to develop our intuition about the possible magnitude of the TCD effect we thus resort to calculating the TCD spectra generated by two simple physical models of the relevant molecular motions.

Mass and spring model. Given the prevalence of helical substructures in terrestrial biopolymers such as proteins, DNA, and RNA (see Discussion), we are compelled to explore a “masses and springs” model of a helical molecular structure as a simple physical representation that captures the essential features of biological macromolecules. Here we eschew as much detail as possible and strive for the simplest model that produces TCD and that we can manipulate to develop some intuition about spectral signatures and their order of magnitude.

Models of vibrational CD have been explored, but these have largely focused on spectra in the near-infrared, spectra dominated by bond stretching and bending, and the wagging of small subunits in a macromolecule (Deutsch and Moscowitz, 1968, 1970; Holzwarth and Chabay, 1972; Schellma, 1973). The terahertz part of the spectrum couples to macromolecular vibrations of the “whole” and requires a model that explores collective vibrations. In collective vibrations nearest neighbor atoms move together, with large relative motions being experienced only by pairs of atoms that are widely separated in the macromolecule. An important consideration is that, as these low-frequency macromolecular vibrations

F1



4C

FIG. 1. The structure of the protein bacteriorhodopsin, a typical example of one of the stereochemically pure, chiral macromolecules universally associated with life on Earth. Shown is a schematic diagram of the protein in which only the backbone of the polymer, a few key side chains, and the optical chromophore are illustrated—were all atoms presented in the figure the protein would appear from the outside to be a well-packed, monolithic structure. Indicated by arrows are the atomic motions involved in the protein's low-frequency mode at 0.498 THz. As is generally the case with the low-frequency vibrational modes of bacteriorhodopsin, this mode involves large amplitude, in-plane motion of its seven α -helices. Our analysis suggests that these low-frequency modes will exhibit significant CD. The length of the arrows is proportional to the motion of the element involved, but is exaggerated to facilitate viewing.

soften, they evolve into large-amplitude conformational changes that are widely held to be biologically (functionally) relevant (e.g., Tama and Brooks, 2002).

Our model comprises a simple collection of masses distributed uniformly in a helical pattern (Fig. 2). Each mass represents more than a simple atom or ion; it represents the covalently bonded atom on the backbone and whatever is attached to it. We assume that these units interact only with their nearest neighbors. For the sake of simplicity we assume all masses are the same, and we treat only the torsional motion of the masses about the axis of the helix (Fig. 2). This model will produce acoustic-like torsional modes that propagate along the helix. The model is further simplified by not considering radial and longitudinal acoustic modes. To couple to the propagating terahertz electromagnetic field and produce a polarization that attenuates and alters the speed of the electromagnetic wave, charge must be distributed along the helix. The

parameters used, which roughly approximate the α -helix of terrestrial proteins, are the following: period of the helix, 0.55 nm; masses/period, 10; charge distribution, $-5e/14$ sites; highest-frequency acoustic mode, 10 THz; volume density or helix period/ m^3 , $0.9 \times 10^{27} m^{-3}$; relaxation time, $0.53 \times 10^{-12} s$.

Normal mode analysis. While simple, generic models can provide important insights into the general issue of macromolecular TCD, it is also important to explore whether similar effects are present in more realistic models of terrestrial biopolymers. To this end we have also performed detailed calculations of the TCD spectra of a specific, representative biopolymer, the archeal protein bacteriorhodopsin (Fig. 1). Normal mode calculations (Brooks *et al.*, 1995) were performed to analyze the low-frequency modes in the native protein [wild type (WT)] and a version of the protein containing a single mutation in which the residue aspartate-96 is replaced with asparagine

F2

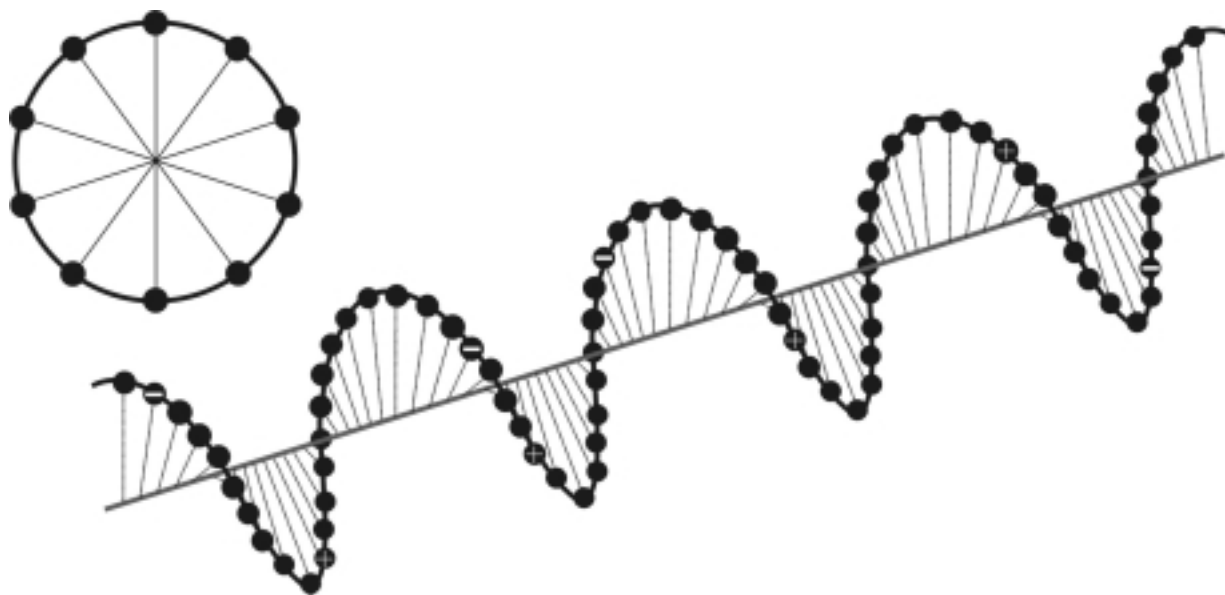


FIG. 2. End and side views of a simple “mass and spring” model that captures the TCD features of a generic, chiral macromolecule. The motion of the masses is described by a simple rotation about the helix axis. The angular motion of neighboring masses is coupled through a restoring torque proportional to the relative rotations. An electromagnetic field forces the charged masses to rotate producing a polarization that can be both in the direction of the field but also normal to it via the mutual coupling.

(D96N). We selected this mutation because of the availability of a crystal structure. The atomic coordinates used in the calculations were PDB entry 1C3W [0.155 nm resolution (Luecke *et al.*, 1999a)] for WT and PDB entry 1C8R [0.20 nm resolution (Luecke *et al.*, 1999b)] for D96N. Hydrogen atoms were added using Insight II (version 2000, Accelrys, San Diego, CA). The protonation states of the residues were assigned following the literature (Ren *et al.*, 2001). The water molecules present in the crystal structure were included in one set of calculations and excluded in a second set of calculations. This approach allows us to determine the impact of biological water on terahertz spectra (Fig. 3).

F3

The crystal structure of a protein is generally inappropriate for direct harmonic analysis, and the structure must be minimized prior to analysis (Janezic and Brooks, 1995; Janezic *et al.*, 1995). We used the program CHARMM (Brooks *et al.*, 1983) to generate a minimum energy structure while applying harmonic constraints to the protein backbone during the initial minimization. The constraints were progressively reduced at each cycle, and then the constraints were removed and the system was minimized until the energy gradient was below 4×10^{-6} kJ/mol. The nonbonded interactions were truncated at 1.3 nm,

and van der Waals interactions switched between 1.0 and 1.2 nm.

Normal modes were obtained using the “Iterative Diagonalization in a Mixed Basis Set” method, which was developed previously to handle large molecular systems (Mouawad and Perahia, 1993). This method uses an iterative procedure that provides good accuracy for the low-frequency regions of interest to this study. The program CHARMM (Brooks *et al.*, 1983; MacKerell *et al.*, 1998) was used for all energy minimizations and normal mode analysis.

The normal modes were determined, and a representative low-frequency mode was selected for further analysis (Fig. 1). Analysis of all the strong modes below 3 THz indicates that the vast majority involve large-amplitude motion of entire helices (similar to those shown in Fig. 1). The intensity of such modes is due to the fact that one or more of the residues in these helices are charged, which generates a large change in dipole moment associated with the vibrational motion. Of particular interest here, however, is the extent to which such vibrations are CD-active. We simulated the TCD spectrum of a protein undergoing large-amplitude motion of helical segments by creating an artificial system containing seven partially charged masses connected via weak

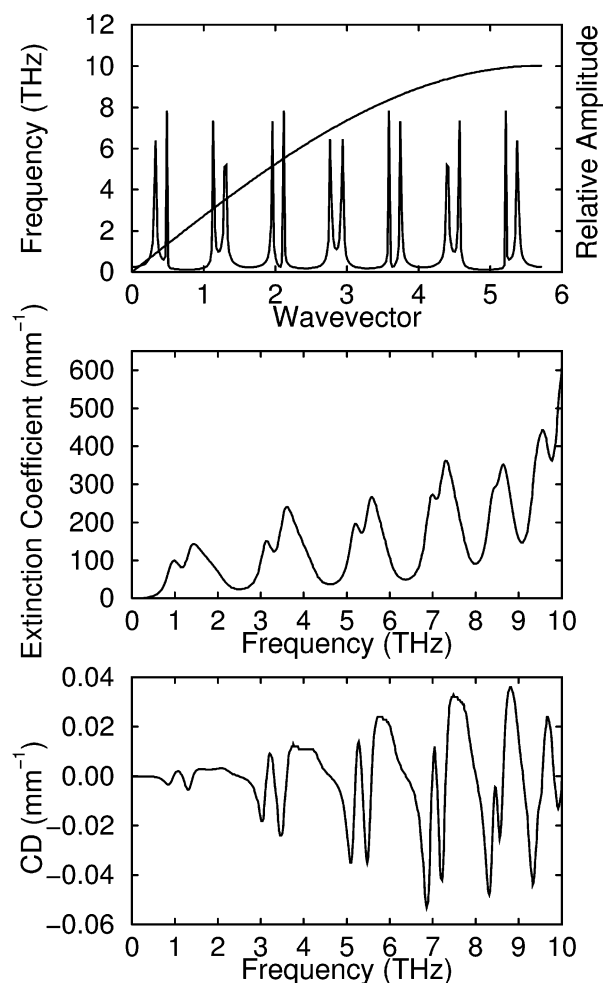


FIG. 3. Calculated terahertz spectra of wild-type bacteriorhodopsin (top) and bacteriorhodopsin modified via single amino acid replacement (bottom; D96N mutation). The contributions of water (dotted line) are highlighted by dividing the spectrum calculated for the protein in the presence of water by that calculated in the absence of water. Both macromolecules absorb strongly and broadly across the terahertz, suggesting that terahertz spectroscopy would be a relatively broad probe of macromolecules in general. Of note, however, the distinct differences between the spectrum of the WT and mutant proteins indicate that the precise details of the spectra depend on the precise details of the molecular structure. Also noteworthy is the observation that water enhances the intensity of all bands, and has a significant effect on the lowest-frequency modes.

bonds. The system was constructed using atoms selected so that a planar equilibrium geometry is obtained, and the system was minimized using Hartree-Fock *ab initio* procedures and a 6-31G(d) basis set. The system was then modified by increasing the masses of the atoms 100-fold to produce resonances that mimic large-amplitude protein vibrations involving entire helix segments

(Fig. 1). The vibrational CD engine within Gaussian-98 was used to predict the TCD spectrum. The physics underlying this approach are well established and well documented, and thus we will not reiterate a detailed discussion of the method here but instead direct interested readers to the relevant literature (Cheeseman *et al.*, 1996; Frisch *et al.*, 1998).

Development of a TCD spectrometer

Sources and detectors. We are currently developing TCD spectrometers based on two terahertz sources: the UCSB Free Electron Laser, a tunable, kilowatt pulsed source covering from 0.12 to 5 THz (Ramian, 1992), and a solid-state, continuous wave (CW), 20 mW Gunn Oscillator operating at 0.14 THz (Quinstar Technology, Inc., Torrance, CA). The Gunn Oscillator is a compact, low-mass, low-power source. It is also a CW source, thus allowing for the rapid modulation of polarization for the purposes of synchronous detection, which can produce potentially critical improvements in signal-to-noise. The free electron laser, in contrast, fills a three-story building (and thus is hardly “flight-ready technology”) and is a non-CW source (repetition rate ~ 3 Hz). Given its high output power and tunability, however, it is an ideal test instrument to explore and document TCD in strongly absorbing material over a broad frequency range. Further, while the terahertz part of the spectrum remains less well developed than either the UV-visible or near-infrared parts of the spectrum, much specialized research instrumentation has been developed, largely for astrophysical applications. Perhaps most promising are recent demonstrations of quantum cascade lasers operating at frequencies as low as 3.4 THz (Williams *et al.*, 2003) suggesting that compact, robust, low-power solid-state terahertz sources will be available within the next few years. In addition to high-power sources, strongly absorbing material will also require the use of sensitive detectors and thus cryogenic hot electron bolometers and photoconductors that are fast and have NEP (noise equivalent input powers per root Hz) $\sim 10^{-12}$ W. The work described here, however, employs less sensitive, but more convenient, room temperature pyroelectric detectors.

Optics for circular polarization. Circular polarization occurs when the phase of the transverse

electric field on one axis is advanced or delayed by 90° with respect to the (equal amplitude) field on the other axis. To an observer, the net electric field vector will appear to rotate, to the left or right depending on which axis is delayed, completing one rotation per wavelength. Linear polarization can be converted to circular, and vice versa, with a birefringent material fabricated as a quarter-wave plate or by using wire grid polarizers that separate two orthogonal polarizations and introduce the appropriate phase delay by a difference in path length. The “purity” of the right or left circular polarization depends on the relative amplitudes of the two phases and is readily assayed (to within a precision of $\sim 1\%$) by rotating a linear polarizer in the beam and, for some spectrometer designs, is easily adjusted (via modulation of the input polarizations). Critically, CD signal strength is linearly related to polarization purity, and thus discrepancies of even a few percent are not a significant hurdle with respect to achieving the qualitative goal of life detection.

The measurement of CD in the visible and near-infrared (500 nm–10 μm) is well established, with a number of excellent commercial instruments available (reviewed by Kliger *et al.*, 1990). In order to generate alternating polarizations these spectrometers generally employ the elastooptic properties to induce birefringence in materials such as ZnSe. A piezo-electric transducer provides sufficient drive for a full polarization cycle. A similar approach cannot be employed at terahertz frequencies, however, because the orders of magnitude longer wavelength would require prohibitively large electromechanical driving of the birefringent material. We are exploring several means of generating alternating circular polarization that appear well suited to the terahertz regime (Fig. 4). Each has unique advantages and disadvantages regarding its modulation rate and its ability to generate pure, stable circular polarization across a broad swath of the terahertz spectrum.

Our first approach (Fig. 4, top) involves a rotating quartz wave plate. This consists of an x -cut (cut parallel to the growth, or z -axis) quartz crystal, which exhibits “slow” and “fast” axes that result in a $1/4 \lambda$ phase shift between vertically and horizontally polarized light. A linearly polarized input beam is passed through the plate, generating an alternating right-circular/linear/left-circular/linear polarized output as the quartz is rotated.

Our second approach (Fig. 4, middle) utilizes

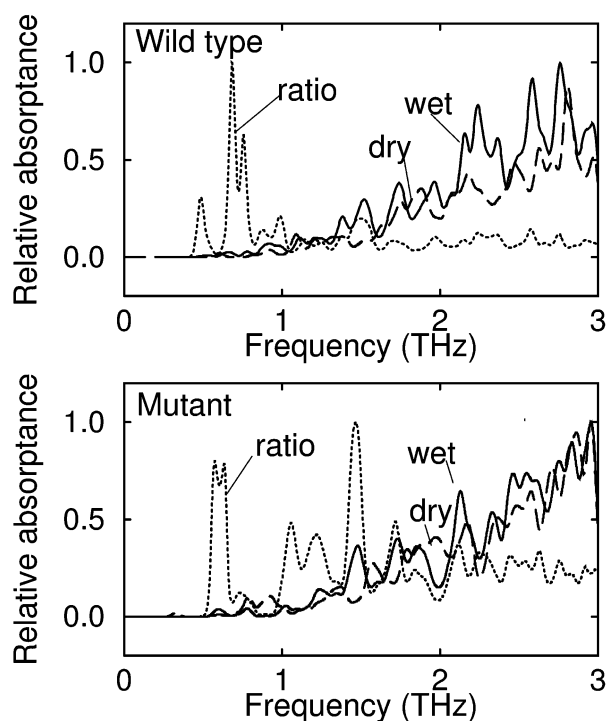


FIG. 4. Schematics and images of TCD spectrometers built using a quartz $1/4$ wave plate (top), rotating polarizers (middle), and moving mirrors (bottom).

a reflective circular polarizer, consisting of a free-standing wire grid placed $1/8 \lambda$ in front of a mirror. Half of the radiation is immediately reflected by the grid, while the other half, in the orthogonal polarization, is reflected by the mirror and delayed by $1/4 \lambda$ resulting in a conversion from linear to circular polarization. A rotating polarizer modulates the incident radiation falling on the circular polarizer, alternating between $+45^\circ$ and -45° with respect to the wire grid and thus generating alternating circular polarizations.

Our third approach (Fig. 4, bottom) uses a polarizing Michaelson interferometer. Wire grid polarizers in each arm are orthogonally oriented. As the length of one arm is changed, the phase relationship between vertical and horizontal components defines a sequence of polarization states including pure left and pure right circular. The mirror is stepped by $1/4$ wavelength to sequentially alternate between left and right circular for each FEL pulse. This approach is especially attractive for continuous sources. Another significant advantage of this approach is that both amplitude and phase can be adjusted in order to provide near-perfect circular polarization.

Samples: the first control experiments. In order to test and debug our initial TCD spectrometer schemes, we have employed small, hand-wound springs of 0.23 mm diameter made from 0.025-mm copper wire. These materials are both conducting and chiral (helical) on dimensions similar to those of the wavelengths being probed and should exhibit very strong CD signals. Because these materials are certain to exhibit strong CD, we have employed “single-handed” samples of such springs, in random orientations, in our positive control experiments.

RESULTS

Arguments, simulation results, and limited experimental data supporting the concept that TCD is an unambiguous and universal approach to life detection are provided in the following sections, as well as a description of progress towards the building of the first TCD spectrometers.

Key assumptions

Enantiomerically pure, chiral macromolecules: a universal signature of life. All living systems, irrespective of their genesis, will employ macromolecular “machines” in order to carry out their metabolic and reproductive functions. A critical component of life, which is defined here as a self-replicating chemical system capable of evolving, is the genetic storage of information (DNA and, to a lesser extent, RNA are the terrestrial analogs). This genetic material must encode the molecular machines that are required to copy itself using as building blocks only raw materials available from the environment (with proteins and, to a lesser extent, RNA playing this role terrestrially). These machines, like all “tools,” are fundamentally three-dimensional objects. Moreover, like the vast majority of three-dimensional objects, these macromolecular machines are chiral. That is, they lack any mirror planes of symmetry and thus are not superimposable onto their mirror images. In particular, the most obvious chiral symmetry in terrestrial biomaterials arises due to the helical substructures that, despite their vastly differing chemistries, are adopted by proteins, DNA, RNA, and polysaccharides (e.g., Fig. 1). It has been argued that the ubiquity of these helical structures reflects unavoidable geometric constraints associated with packing a polymer into a compact ob-

ject (e.g., Yee *et al.*, 1994; Maritan *et al.*, 2000; Stasiak and Maddocks, 2000).

Evolution, a critical component of the definition of life, will produce selective pressures that ensure that these chiral, biologically produced macromolecules will be produced in enantiomerically pure (only one stereoisomer) form. This is because, by analogy to the observation that your right shoe does not fit on your left foot, in general only one of the two enantiomers will be biologically active. The production of the incorrect, inactive enantiomer is thus almost always wasteful, and its elimination will be the subject of selective pressures. [Pursuing the above analogy, if evolution had invented footwear, there would be selective pressure to suppress the asymmetry between our feet in order to avoid wasting the resources required to maintain separate pathways for the synthesis of both left and right shoes. In molecular systems such as asymmetries cannot be suppressed—chirality is a fundamental characteristic of any intermolecular interaction that utilizes three or more “attachment points” for recognition (Ogston, 1948)—and thus, at the molecular level, the inevitable outcome of this selection is homochirality rather than achirality.] Terrestrially, the symmetry between right- and left-handed macromolecules is perfectly and universally broken by the use of homochiral monomers in the synthesis of proteins, DNA, RNA, and polysaccharides. (Polymers composed of achiral monomers also fold into chiral objects but, in contrast, exhibit no net chirality because they populate both enantiomers equally.) Chiral, macromolecular machinery should thus provide a universal signature of chemical life, irrespective of its genesis.

How common are chiral macromolecules in living organisms? We cannot, of course, know the ultimate limits on this value, but considering the numbers for a typical terrestrial example would seem a reasonable first approximation. The common bacterium *Escherichia coli* is composed of, by mass, 70% water, 15% protein, 7% RNA and DNA, 3% polysaccharides, 2% lipids, and 3% inorganic ions and small molecule metabolites (Ingraham *et al.*, 1983). Of note, about 5% of the water is physically coupled to chiral macromolecules in the form of an inner hydration shell, and our calculations indicate that this material behaves as if it were part of the macromolecule (see below). Thus approximately 30% of the mass of a typical terrestrial cell is composed of chiral macromolecules

or is chiral by close physical association with such macromolecules. Given the abundance of chiral macromolecules and their argued association with life irrespective of its chemical genesis, the important remaining questions are whether chiral macromolecules are an unambiguous signature of life and whether there exists a feasible, *unbiased* means of detecting them.

Chiral macromolecules are an unambiguous signature of life. It is widely held that enantiomerically pure (i.e., net chiral) materials unambiguously distinguish biological material from abiological material (e.g., MacDermott *et al.*, 1996; MacDermott, 1997). And while most of the support for this assertion is, in a sense, *negative* observations, the large body of these observations argues strongly that the postulate is well founded. For example, motivated by the observation that all terrestrial organisms use the L enantiomers of the amino acids and the D enantiomers of ribose or deoxyribose in RNA and DNA, many creative theories have been explored in an effort to explain these homochiral “choices” in terms of enantiomeric biases predating the origins of life. Hypothesized mechanisms range from stereoselective destruction of small molecules by circularly polarized UV light from magnetic neutron stars (reviewed by Bailey, 2000; Jorissen and Cerf, 2002), through the influence of parity violation in the weak nuclear force (reviewed by Podlech, 2001), to the influence of the “handedness” of the Earth’s orbit around the sun (e.g., He *et al.*, 2000). Despite serious effort, however, only the first of these mechanisms has ever been reported to produce any net chirality in the laboratory, and even then the enantiomeric excess never exceeds a few percent under even the most extreme experimental conditions (e.g., Bailey, 2000; Keszthelyi, 2001; Podlech, 2001; Wang and Liang, 2001). And while beaker-scale syntheses have been reported that employ vigorous stirring (e.g., Kondepudi and Sabanayagam, 1994) to generate net chirality (apparently by crushing and mixing the first nucleating crystal and thus ensuring that all subsequent crystals nucleate with the same handedness), either enantiomer is equally likely to be produced in any given repeat of the experiment, and thus this effect is extremely unlikely to generate net chirality on a planetary scale (reviewed by Podlech, 2001). That said, a minor (2–9%), presumably abiologically produced enantiomeric excess has been observed in an astronomical con-

text (e.g., Pizzarello and Cronin, 2000), though the mechanisms underlying these minor excesses have not been identified. In contrast, it is well established that minor enantiomeric excesses such as these are insufficient to generate the homochiral, folded *heteropolymers* associated with life (e.g., Bonner, 1995; Brandon and Tooze, 1999). It appears, instead, that planetary-scale homochirality—net chirality of sufficient magnitude to generate chiral macromolecules—can only occur when small-scale chiral fluctuations (randomly generated or biased by mechanisms such as those described above) are amplified via evolutionary selection. For this reason we, and many others (e.g., MacDermott *et al.*, 1996; MacDermott, 1997), believe that the observation of net chirality is an unambiguous signature of biological processes.

Chiral macromolecules exhibit TCD. Extensive simulations, theory, and empirical observations suggest that all polar macromolecules, irrespective of their chemistry, will exhibit collective vibrational modes that are terahertz-active. If the macromolecules are net chiral, these modes will produce TCD. The significant question remains, however, as to whether the TCD signals thus produced intense enough to be readily measured. Here we explore these issues with reference to the literature and to simulations.

All polar macromolecules absorb strongly in the terahertz. Extensive molecular dynamics simulations (e.g., Brooks and Karplus, 1985; Hinsen, 1998; van Vlijmen and Karplus, 1999; Hinsen *et al.*, 2000; Tama *et al.*, 2000), normal mode calculations (e.g., Chen and Prohofsky, 1995; de Groot *et al.*, 1998; Hery *et al.*, 1998; Buck and Karplus, 1999), and more limited experimental studies (e.g., Markelz *et al.*, 2000; Globus *et al.*, 2002; Woolard *et al.*, 2002) indicate that effectively all biomolecules of >500 atoms absorb strongly in the terahertz because of collective vibrational modes. It is this combination of broad absorption at terahertz frequencies and the potential for attendant broad CD (see below) occurring almost irrespective of the chemistry of the biomolecule that makes the terahertz part of the spectrum attractive as an unbiased (in terms of the precise chemistry of the molecular machinery involved) vehicle for life detection.

All chiral macromolecules will exhibit CD at terahertz frequencies. CD, which is the wavelength-specific differential absorption of left and right

circularly polarized light, provides information on the asymmetry of chromophores. The optical (UV, visible, near-infrared) chromophores of the first row elements (i.e., elements that make strong covalent bonds and are likely components of life: carbon, oxygen, etc.), however, are achiral (e.g., carbonyls, carbon-carbon double bonds, etc.) and thus do not inherently exhibit CD. When they are present in a chiral, structured biomolecule, however, they are typically placed into asymmetric environments or participate in asymmetric exciton interactions and thus exhibit CD. Because optical CD provides information on the structure of biopolymers, the technique is an integral part of contemporary biophysics, and numerous, excellent turnkey instruments are commercially available (reviewed by Kliger *et al.*, 1990).

While optical CD is an extremely well-established technique, the approach has several drawbacks as a general life-detection scheme. For example, the use of optical CD assumes that the putative biomaterial in question contains strong optical chromophores. While such chromophores are relatively common, the assumption that all life forms will utilize heteropolymers absorbing at optical wavelengths should be avoided if possible. A related concern regarding optical CD is that by far the most likely chromophores in biological materials are composed of the cosmologically abundant, strongly covalent first row elements hydrogen, carbon, nitrogen, and oxygen, and the optical chromophores of these structures generally produce only weak CD at optical wavelengths. In the UV-visible spectral region, by far the most likely chromophores are electronic transitions of carbon-, nitrogen-, and/or oxygen-containing double bonds. Double bonds of first row elements are inherently symmetric structures, and thus they generally exhibit CD only as a second-order effect when they are placed in asymmetric environments or exhibit asymmetric exciton interactions with other chromophores. These second-order CD effects produce $\Delta\epsilon/\epsilon$ of typically 10^{-3} – 10^{-4} (e.g., Sprecher and Johnson, 1977). In the near-infrared, where likely chromophores are bond vibrations, the chiral asymmetry is even less intrinsic to the system, leading to $\Delta\epsilon/\epsilon$ of 10^{-4} – 10^{-5} for both proteins (e.g., Pancoska *et al.*, 1989) and DNA (e.g., Keiderling *et al.*, 1989).

Because all macromolecules containing charges or polarized bonds absorb in the terahertz, and all chiral macromolecules will exhibit CD, almost all biologically produced macromolecules will

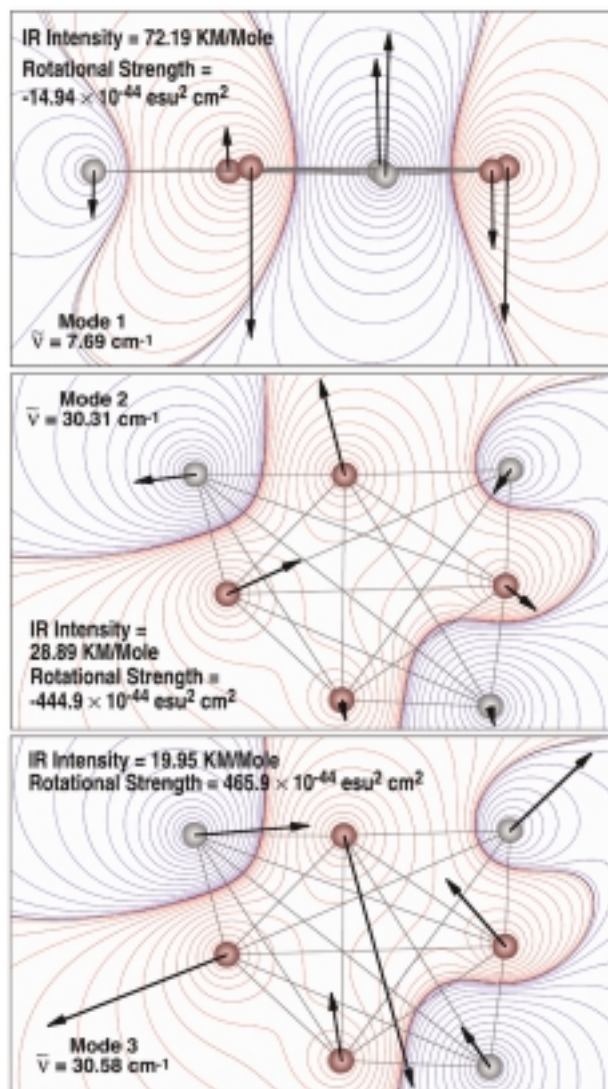
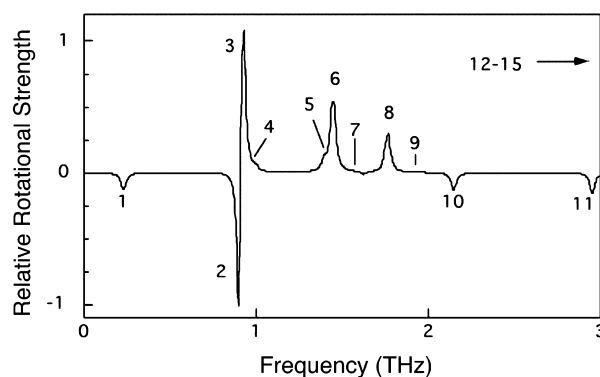


FIG. 5. Top: Dispersion relation for torsional acoustic modes of the model helix. The amplitude versus drive frequency, or wavevector, for the particular charge distribution in the model helix. **Middle:** The absorption spectrum of the model helix. **Bottom:** The model's corresponding CD features, defined as the difference between the extinction of right and left circularly polarized radiation.

produce TCD. The question remains, however, as to whether this TCD is intense enough that it can be readily measured. A simple argument suggesting that the magnitude of TCD may be relatively large is the observation that, in the terahertz, the “chromophores” are the inherently asymmetric macrovibrational modes of chiral objects. At optical wavelengths, where the vast majority of likely chromophores are inherently *symmetric*, the rare occurrence of inherent *asymmetry* leads to 1–2 orders of magnitude larger CD intensities; for example, the inherently asymmetric hydrocarbon hexahelicene exhibits a $\Delta\epsilon/\epsilon$ approaching 1% (Newman *et al.*, 1967).

Simulation results

We have attempted to develop more quantitative insights into the nature and magnitude of biomolecular TCD signals by computing the TCD spectra of two simple, computational models. Both models suggest that macromolecular vibrations of the helical structures inside typical biomolecules will lead to reasonably strong TCD, with precise spectral signatures that are a sensitive function of the distribution of mass, charge, and elastic couplings within the structure.

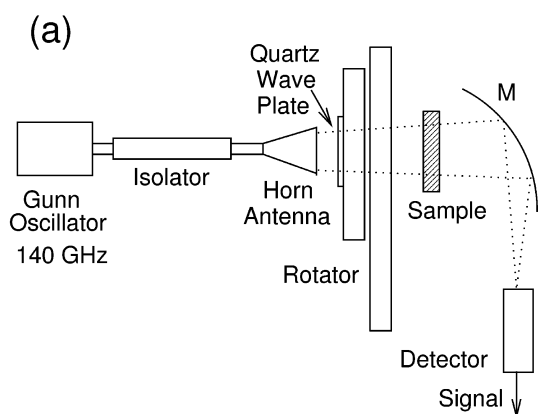
Mass and spring model. CD at terahertz frequencies involves a very different set of excitations than those responsible for UV, visible, and near-infrared CD. UV CD and visible light CD are intimately related to electronic excitations. Near-infrared CD is largely connected to vibrations associated with the stretching and bending of bonds (Deutsche and Moscovitz, 1968, 1970; Schellma, 1973). But excitations in the terahertz and associated CD are best described as macromolecular vibrations involving large pieces of the molecule beating against each other (Fig. 1). In order to simulate such motions, and the TCD spectral features associated with them, we have developed and characterized a simple “mass and spring” model of a typical biopolymer helix. The torsional acoustic modes supported by our specific model of the helix are shown (Fig. 5). As in linear chain models of acoustic modes in solids, the highest-frequency mode corresponds to an acoustic wavelength of $\lambda_{\max} = 2a$, twice the site spacing. This particular calculation assumes that the helix is infinitely long. A finite helix will support additional standing waves with wavelengths determined by the boundary conditions at the ends. If,

guided by typical terrestrial examples (e.g., Fig. 1), we take the helix to be 7 periods long we estimate that the longest wavelength is approximately $\lambda_{\max} = 140a$, corresponding to a frequency of ~ 0.5 THz.

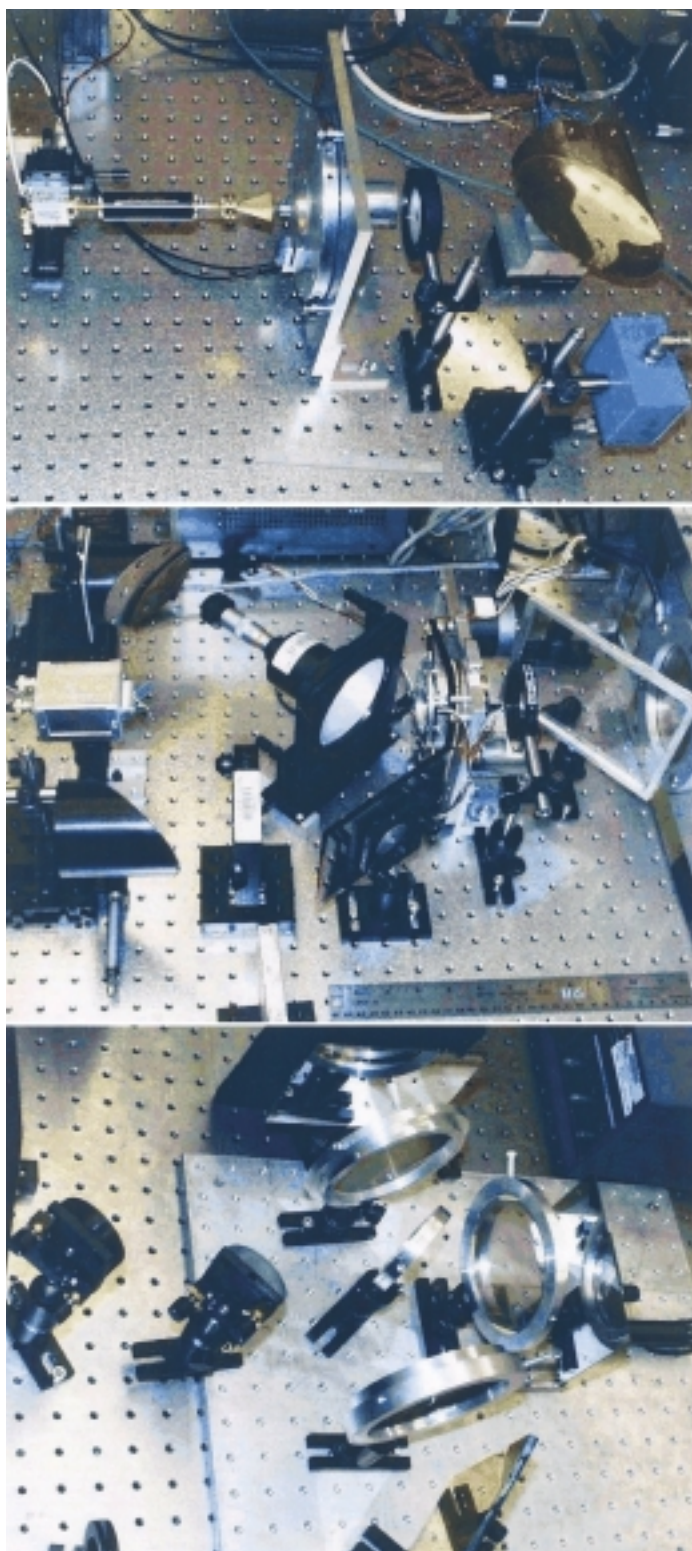
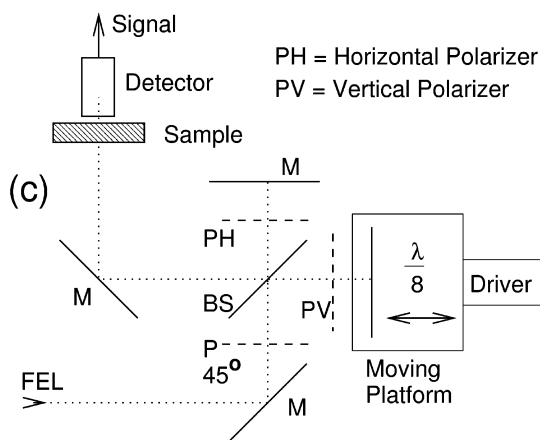
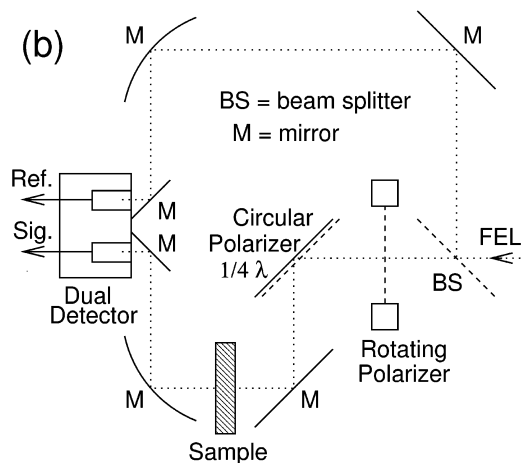
In reality, the excitation of the helix in the biomolecule is not uniform; there are a variety of masses, extraneous coupling to the environment, different charges, and different local field corrections. The electromagnetic field, very nearly uniform on the length scale of the helix, drives a variety of modes determined by the Fourier transform of the charge coupling parameters along the helix. Here we have simply lumped a charge every 14 sites to simulate a very nonuniform excitation of the helix. The consequences of this particular distribution of charge are shown (Fig. 5). The electromagnetic field at a given frequency will resonate with a torsional acoustic mode at a wavevector determined by the dispersion relation, but produces an amplitude exhibiting resonant behavior at acoustic wavelengths or wavevectors determined by the spatial variation of the charge in the helix. We conclude that a particular helix will have a signature determined by, among other things, the distributions of mass and charge.

We have calculated the polarization produced by a linearly polarized electromagnetic wave and find that in addition to the polarization in the direction of the applied terahertz electric field, the system produces polarization perpendicular to it and with the symmetry properties (Fowles, 1989) required to produce rotation or TCD. Several relevant features are observed in the resulting resonant absorption and resonant TCD. As expected, the helical model absorbs strongly at the frequencies corresponding to the resonant excitation shown (Fig. 5, middle). For the model density, the absorption is quite strong. Indeed, it is well known that glasses with reasonable charge density, such as sodium silicate glasses, exhibit strong terahertz absorption that strengthens with increasing frequency. The TCD spectral features consist of a series of zero crossings (Fig. 5, bottom). In the simple model the resonant features are simply determined by the distribution of charges. We may expect that any particular helical unit exhibits a unique, broad band “signature” pattern of such zero crossings.

CD is always a small fraction of the direct absorption. Using visible, UV, or infrared ratios as a guide we would expect that the ratio will be



P = Polarizer
 M = Mirror
 BS = Beam Splitter



4C

FIG. 6. Top: Simulation of the CD spectrum of an artificial bacteriorhodopsin-like system containing seven partially charged point masses connected via weak harmonic bonds (see text). This artificial chiral system generates 15 vibrational modes, the first three of which are illustrated (**lower panels**). Electrostatic contours show the partial charges on the point masses and the arrows indicate relative motion of the masses during the vibration. The rotatory strengths were calculated using the VCD engine within Gaussian-98 (Frisch *et al.*, 1998).

$\sim a/\lambda_{\text{THz}}$, where a is of the order of the atom or ion spacing. This is a very small number at terahertz frequencies. But the molecular unit, the “terahertz chromophore,” that is responsible for the terahertz absorption involves many atoms and ions (Holzwarth and Chabay, 1972). For a helix 7 periods in length, the long wavelength acoustic mode in our simple model is $\sim 140a$, and we expect to recover CD to absorption ratios that are reasonable relative to those of electronic excitations or near-infrared vibrations. For this particular, rather simple model we find $\Delta\epsilon/\epsilon \sim 10^{-4}$, suggesting that TCD may be at least as intense as CD at optical wavelengths. We thus conclude that the collective vibrations of the helical structures inside typical biomolecules are likely to lead to reasonably strong and complex TCD spectra.

Normal mode analysis. We have also performed more detailed calculations to model a specific, representative terrestrial biopolymer, the protein bacteriorhodopsin (Fig. 1). Because bacteriorhodopsin, an archeal light-transducing protein (Oesterhelt and Stoeckenius, 1971), is thought to have been an important contributor to terrestrial life for nearly 3.5 billion years it is perhaps a particularly appropriate choice for this study (Stuart and Birge, 1996). The Archaea from which it is obtained, *Halobacterium salinarum*, is an extreme halophile that lives in natural environments such as the Dead Sea, the Great Salt Lake, or salt flats where the salt concentration is above that found in the oceans (as high as 25% NaCl). The deep purple color of many salt flats is due to high concentrations of this protein in the membrane of these organisms.

As described above, we have simulated the low-frequency vibrational modes of bacteriorhodopsin. There are a total of 268 calculated modes below 3 THz, roughly 20% of which are strongly allowed. The most intense modes involve concerted motions of entire helices, a representative example of which is illustrated (Fig. 1). We simulate the TCD activity of these modes using charged heavy masses to simulate entire helices connected by harmonic springs (Fig. 6). Only some of the resultant modes are reflective of the modes observed in a protein. For example, the lowest-frequency mode (mode 1) is an out-of-plane distortion that has no direct analogy in the bands calculated for bacteriorhodopsin. In contrast, modes 2 and 3 of our simulation have much in common with the in-plane helix translocation

modes that characterize the terahertz vibrations in bacteriorhodopsin. The fact that such modes consistently yield intense TCD bands is logical because the charged unit is vibrating within a chiral arrangement. Based on these simulations we propose that a majority of the strong protein vibrational modes below 3 THz will have observable TCD activity with rotatory strengths in the range 10^{-42} – 10^{-41} esu² cm² (10^{-65} – 10^{-64} C² m²). However, the fact that individual modes have TCD activity does not guarantee that the net TCD spectrum of the biomolecule will be intense. This observation follows from the fact that two nearby modes can have similar but opposite rotational strengths (e.g., modes 2 and 3 in Fig. 6). As the density of vibrational modes increases, the probability of accidental cancellations of net rotational strength will increase. Our simulations indicate that the density of modes increases as the vibrational energy increases, and it is possible that large proteins may yield such a high density of TCD modes above 2 THz that the average rotational strength will start to decrease at energies near or above this frequency. A definitive answer to this hypothesis is beyond the capability of our current models and thus provides further impetus for experimental studies of TCD.

“Induced chirality” in macromolecular hydration shells. We have also investigated the contributions of hydration shells to likely biomolecular TCD signatures. Although water is the principal constituent of biological systems, it is achiral, and thus bulk water will not exhibit TCD. Approximately 1–5% of the water in a cell, however, is “biological water” that is in direct association with polar or charged groups on the surface or inside of proteins and nucleic acids and may, due to this “induced chirality,” be CD-active. In order to test this, we have carried out a series of calculations on biological water using Hartree-Fock and density functional (B3LYP) methods. We were surprised to find that, by weight, biological water will likely be the single most important source of a TCD signature of a hydrated biological system. We find two sources of contribution. The first is solvation enhancement. When water is added to a system, it stabilizes ionic species through direct association with the polar and charged amino acids. When these residues participate in low-frequency, large-amplitude vibrational motion, the hydration shell moves to maintain stabilization of the polar or charged species.

F6

The net result is a lowering of the frequency and an enhancement in the intensity of the signal. The frequency is lowered because the mass of the vibrating system has increased. The intensity increases because the magnitude of the charges is enhanced through solvation. Because a chiral subsystem imparts chirality on the supersystem, the first hydration shell enhances the chirality of the local protein environment. The second hydration shell tends to slightly diminish the chirality because of fluid motion, and subsequent shells have relatively little impact. In all cases we investigated, however, water enhanced the TCD signature. We also found that there were some specific cases of very intense TCD signals associated with water “wires” that bridged the gap between two charged residues. In the five examples studied, water wires containing from three to seven molecules exhibited low-frequency modes in the 0.3–3 THz region, and many of these modes had rotatory strengths above 10^{-42} esu² cm². From a mass-weighted perspective, water wires between charged residues were the single most important source of TCD bands that we observed in our simulations.

Development of TCD spectrometers

Previous attempts to build TCD spectrometers have met with only limited success (Polavarapu and Chen, 1994; Polavarapu and Deng, 1996). We are currently developing three competing TCD spectrometer schemes (Fig. 4) that potentially offer significant advantages over previous efforts in terms of both signal-to-noise ratios and possible systematic errors. The three approaches differ in the manner in which alternating circular polarization is generated.

TCD appears technologically feasible. To date the most progress has been made with a spectrometer that generates alternative polarizations via a quartz $1/4 \lambda$ wave plate. Because quartz crystals are birefringent, the indices of refraction for vertically and horizontally polarized light differ at terahertz wavelengths, an effect that can be used to construct a $1/4 \lambda$ wave plate that generates alternating right- and left-circularly polarized light as the quartz is rotated (Fig. 4, top panels). The signal-to-noise ratio of the currently implemented (manually operated and thus with limited averaging) spectrometer is $\sim 10^2$. While this is insufficient to detect TCD in terrestrial bioma-

terials, it is sufficient to detect the TCD arising from small metal springs, which are both conducting and chiral on the length scale of the radiation and thus exhibit strong CD (Fig. 7). We anticipate that, with the inclusion of reference detectors, antireflective coatings, significant, automated signal averaging, and, ultimately, synchronous detection, it will be possible to improve the signal-to-noise of this spectrometer to the $\sim 10^5$ we estimate would be suitable for a life-detection approach.

DISCUSSION

Here we have argued that, irrespective of the chemistry upon which they are based, all forms of chemical life will employ enantiomerically pure, chiral macromolecules as the “machines” employed in their metabolism and reproduction. The results of our simulations strongly suggest that all such macromolecules will absorb strongly in the terahertz, as has been previously documented experimentally for terrestrial biopolymers, and that these absorbance features will exhibit relatively strong CD. There appear to be

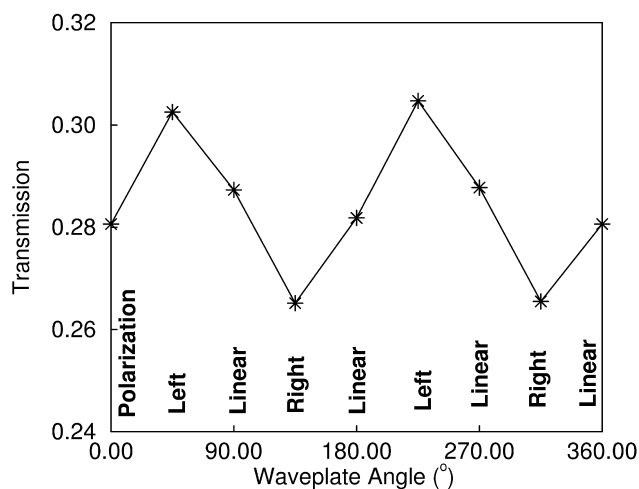


FIG. 7. TCD signals of 0.23-mm-diameter, right-handed, copper springs observed at 0.14 THz using the rotating quartz $1/4$ waveplate spectrometer. The reproducibility of measurements, collected at 180° intervals, clearly demonstrates the impressive signal-to-noise obtained with this spectrometer despite the relatively minor averaging used in this data collection (each point represents eight replicates). The non-equivalence of the observed transmittance of linearly polarized radiation at 90° intervals reflects the small linear dichroism associated with these (imperfectly helical) springs.

several possible means of building a spectrometer to detect this TCD, one of which we have built and used to have measure the TCD of a macroscopic, positive control. The TCD life-detection approach not only provides a potential test for chirality as a signature of life in unknown, complex materials, but also serves to highlight the much broader and hitherto poorly explored concept of detecting life via the macromolecular machinery with which it carries out its metabolic and genetic functions.

ACKNOWLEDGMENTS

Funding for the University of California, Santa Barbara portions of this research program were provided by NASA (NAG5-12150) and the ARO (DAAD19-02-01-0080), and for the University of Connecticut group from the NIH (GM-34548) and NSF (EIA-0129731).

ABBREVIATIONS

CD, circular dichroism; CW, continuous wave; PAH, polycyclic aromatic hydrocarbon; TCD, terahertz circular dichroism; WT, wild type.

REFERENCES

- Anbar, A.D., Roe, J.E., Barling, J., and Neelson, K.H. (2000) Nonbiological fractionation of iron isotopes. *Science* 288, 126–128.
- Bailey, J. (2000) Chirality and the origin of life. *Acta Astronaut.* 46, 627–631.
- Bonner, W.A. (1995) Chirality and life. *Origins Life Evol. Biosphere* 25, 175–190.
- Brandon, C. and Tooze, J. (1999) *Introduction to Protein Structure*, 2nd edit., Garland Publishing, New York, p. 5.
- Brooks, B. and Karplus, M. (1985) Normal modes for specific motions of macromolecules: application to the hinge bending mode of lysozyme. *Proc. Natl. Acad. Sci. USA* 82, 4995–4999.
- Brooks, B.R., Bruccoleri, R.E., Olafson, B.D., States, D.J., Swaminathan, S., and Karplus, M. (1983) CHARMM: a program for macromolecular energy, minimization, and dynamics calculations. *J. Comput. Chem.* 4, 187–217.
- Brooks, B.R., Janezic, D., and Karplus, M.K. (1995) Harmonic analysis of large systems. I. Methodology. *J. Comput. Chem.* 16, 1522–1542.
- Buck, M. and Karplus, M. (1999) Internal and overall peptide group motion in proteins: molecular dynamics simulations for lysozyme compared with results from X-ray and NMR spectroscopy. *J. Am. Chem. Soc.* 121, 9645–9658.
- Cheeseman, J.R., Frisch, M.J., Devlin, F.J., and Stephens, P.J. (1996) *Ab initio* calculation of atomic axial tensors and vibrational rotational strengths using density functional theory. *Chem. Phys. Lett.* 252, 211–220.
- Chen, Y.Z. and Prohofsky, E.W. (1995) Sequence and temperature dependence of the interbase hydrogen-bond breathing modes in B-DNA polymers. Comparison with low-frequency Raman peaks and their role in helix melting. *Biopolymers* 35, 573–582.
- de Groot, B.L., Hayward, S., van Aalten, D.M.F., Amadei, A., and Berendsen, H.J.C. (1998) Domain motions in bacteriophage T4 lysozyme: a comparison between molecular dynamics and crystallographic data. *Proteins* 31, 116–127.
- Deutsche, C.W. and Moscovitz, A. (1968) Optical activity of vibrational origin. I. A model helical polymer. *J. Chem. Phys.* 49, 3257–3272.
- Deutsche, C.W. and Moscovitz, A. (1970) Optical activity of vibrational origin. II. Consequences of polymer conformation. *J. Chem. Phys.* 53, 2630–2635.
- Fowles, G.R. (1989) *Introduction to Modern Optics*, 2nd edit., Dover Publications, New York.
- Frisch, M.J., Trucks, G.W., Schlegel, H.B., Scuseria, G.E., Robb, M.A., Cheeseman, J.R., Zakrzewski, V.G., Montgomery, J.A., Stratmann, R.E., Burant, J.C., Dapprich, S., Millam, J.M., Daniels, A.D., Kudin, K.N., Strain, M.C., Farkas, O., Tomasi, J., Barone, V., Cossi, M., Cammi, R., Mennucci, B., Pomelli, C., Adamo, C., Clifford, S., Ochterski, J., Petersson, G.A., Ayala, P. Y., Cui, Q., Morokuma, K., Malick, D.K., Rabuck, A.D., Raghavachari, K., Foresman, J.B., Cioslowki, J., Ortiz, J.V., Stefanov, B.B., Liu, G., Liashenko, A., Piskorz, P., Komaromi, I., Gomperts, R., Martin, R.L., Fox, D.J., Keith, T., Al-Laham, M.A., Peng, C.Y., Nanayakkara, A., Gonzalez, C., Challacombe, M., Gill, P.M.W., Johnson, B.G., Chen, W., Wong, M.W., L. Andres, J., Head-Gordon, M., Replogle, E.S., and Pople, J.A. (1998) *Gaussian 98*, Gaussian, Inc., Pittsburgh.
- Globus, T.R., Woolard, D.L., Samuels, A.C., Gelmont, B.L., Hesler, J., Crowe, T.W., and Bykhovskaia M. (2002) Submillimeter-wave Fourier transform spectroscopy of biological macromolecules. *J. Appl. Phys.* 91, 6105–6113.
- Greenwood, J.P., Riciputi, L.R., and McSween, H.Y. (1997) Sulfide isotopic compositions in shergottites and ALH84001, and possible implications for life on Mars. *Geochim. Cosmochim. Acta* 61, 4449–4453.
- He, Y.J., Qui, F., and Qi, S.D. (2000) Effect of Earth's orbital chirality on elementary particle and unification of chiral asymmetries in life on different levels. *Med. Hypotheses* 54, 783–785.
- Henning, T.H. and Schnaiter, M. (1998) Carbon—from space to laboratory. *Earth Moon Planets* 80, 179–207.
- Hery, S., Genest, D., and Smith, J.C. (1998) X-ray diffuse scattering and rigid-body motions in crystalline lysozyme probed by molecular dynamics simulation. *J. Mol. Biol.* 279, 303–319.
- Hinsen, K. (1998) Analysis of domain motions by ap-

- proximate normal mode calculations. *Proteins* 33, 417–429.
- Hinsen, K., Petrescu, A.J., Dellerue, S., Bellissent-Funel, M.C., and Kneller, G.R. (2000) Harmonicity in slow protein dynamics. *Chem. Phys.* 261, 25–37.
- Holzwarth, G. and Chabay, I. (1972) Optical activity of vibrational transitions: a coupled oscillator model. *J. Chem. Phys.* 57, 1632–1634.
- Ingraham, J.L., Maaløe, O., and Neidhardt, F.C. (1983) *Growth of the Bacterial Cell*, Sinauer Associates, Sunderland, MA.
- Janezic, D. and Brooks, B.R. (1995) Harmonic analysis of large systems. II. Comparison of different protein models. *J. Comput. Chem.* 16, 1543–1553.
- Janezic, D., Venable, R.M., and Brooks, B.R. (1995) Harmonic analysis of large systems. III. Comparison with molecular dynamics. *J. Comput. Chem.* 16, 1554–1566.
- Jorissen, A. and Cerf, C. (2002) Asymmetric photoreactions as the origin of biomolecular homochirality: a critical review. *Origins Life Evol. Biosphere* 32, 129–142.
- Keiderling, T.A., Yasui, S.C., Pancoska, P., Dukor, R.K., and Yang, L. (1989) Biopolymer conformational studies with vibrational circular dichroism. *SPIE Proc.* 1057, 7–14.
- Keszthelyi, L. (2001) Homochirality of biomolecules: counter-arguments against critical notes. *Orig. Life Evol. Biosphere* 31, 249–256.
- Klein, H.P. (1974) Automated life-detection experiments for Viking mission to Mars. *Origins Life* 5, 431–441.
- Klein, H.P. (1992) The Viking biology experiments: epilogue and prologue. *Orig. Life Evol. Biosphere* 21, 255–261.
- Kliger, D.S., Lewis, J.W., and Randall, C.E. (1990) *Polarized Light in Optics and Spectroscopy*, Academic Press, San Diego.
- Kondepudi, D.K. and Sabanayagam, C. (1994) Secondary nucleation that leads to chiral symmetry breaking in stirred crystallization. *Chem. Phys. Lett.* 217, 364–368.
- Luecke, H., Schobert, B., Richter, H.-T., Carttailler, J.-P., and Lanyi, J.K. (1999a) Structural changes in bacteriorhodopsin during ion transport at 2 Å resolution. *Science* 286, 255–260.
- Luecke, H., Schobert, B., Richter, H.-T., Carttailler, J.-P., and Lanyi, J.K. (1999b) Structure of bacteriorhodopsin at 1.55 Å resolution. *J. Mol. Biol.* 291, 899–911.
- MacDermott, A.J. (1997) Exochirality in the solar system and beyond. In *Exobiology: Matter, Energy and Information in the Origin and Evolution of Life in the Universe*, edited by J. Chela-Flores and F. Raulin, Kluwer Academic Press, Amsterdam, pp. 327–332.
- MacDermott, A.J., Barron, L.D., Brack, A., Buhse, T., Drake, A.F., Emery, R.J., Gottarelli, G., Greenberg, J.M., Haberle, R., Hegstrom, A., Hobbs, K., Kondepudi, D.K., McKay, C.P., Moorbath, S., Raulin, F., Sandford, M.C.W., Schwartzman, D.W., Thiemann W., and Tranter, G.E. (1996) Homochirality as the signature of life: the SETH Cigar. *Planet. Space Sci.* 44, 1441–1446.
- MacKerell, A.D., Jr., Bashford, D., Bellott, R.L., Dunbrack, R.L., Jr., Evanseck J.D., Field, M.J., Fischer, S., Gao, J., Guo, H., Ha, S., Joseph-McCarthy, D., Kuchnir, L., Kuczera, K., Lau, F.T.K., Mattos, C., Michnick, S., Ngo, T., Nguyen, D.T., Prodhom, B., Reiher, W.E., III, Roux, B., Schlenkrich, M., Smith, J.C., Stote, R., Straub, J., Watanabe, M., Wiorkiewicz-Kuczera, J., Yin, D., and Karplus, M. (1998) All-atom empirical potential for molecular modeling and dynamics studies of proteins. *J. Phys. Chem. B* 102, 3586–3616.
- Maritan, A., Micheletti, C., Trovato, A., and Banavar, J.R. (2000) Optimal shapes of compact strings. *Nature* 406, 287–290.
- Markelz, A.G., Roitberg, A., and Heilweil, E.J. (2000) Pulsed terahertz spectroscopy of DNA, bovine serum albumin and collagen between 0.1 and 2.0 THz. *Chem. Phys. Lett.* 320, 42–48.
- McKay, C.P. (1998) The search for extraterrestrial biochemistry on Mars and Europa. In *Exobiology: Matter, Energy and Information in the Origin and Evolution of Life in the Universe*, edited by J. Chela-Flores and F. Raulin, Kluwer Academic Press, Amsterdam, pp. 219–227.
- McKay, D.S., Gibson, E.K., Thomas-Keperta, K.L., Vali, H., Romanek, C.S., Clemett, S.J., Chillier, X.D.F., Maechling, C.R., and Zare, R.N. (1996) Search for past life on Mars: possible relic biogenic activity in Martian meteorite ALH84001. *Science* 273, 924–930.
- Mojzsis, S.J. and Arrhenius, G. (1998) Phosphates and carbon on Mars: exobiological implications and sample return considerations. *J. Geophys. Res.* 103, 28495–28511.
- Mouawad, L. and Perahia, D. (1993) Diagonalization in a mixed basis: a method to compute low-frequency normal modes for large macromolecules. *Biopolymers* 33, 599–611.
- National Research Council (2002) *Signs of Life; A Report Based on the April 2000 Workshop on Life Detection Techniques*, National Academy Press, Washington, DC.
- Newman, M.S., Darlak, R.S., and Tsai, L. (1967) Optical properties of hexahelicene. *J. Am. Chem. Soc.* 89, 6191–6193.
- Oesterhelt, D. and Stoekenius, W. (1971) Rhodopsin-like protein from the purple membrane of *Halobacterium halobium*. *Nature* 233, 149–152.
- Ogston, A.G. (1948) Interpretation of experiments on metabolic processes, using isotopic tracer elements. *Nature* 162, 963–963.
- Pancoska, P., Yasui, S.C., and Keiderling, T.A. (1989) Enhanced sensitivity to conformation in various proteins—vibrational circular dichroism results. *Biochemistry* 28, 5917–5923.
- Pizzarello, S. and Cronin, J.R. (2000) Non-racemic amino acids in the Murray and Murchison meteorites. *Geochim. Cosmochim. Acta* 64, 329–338.
- Podlech, J. (2001) Origin of organic molecules and biomolecular homochirality. *CMLS Cell. Mol. Life Sci.* 64, 329–338.
- Polavarapu, P.S. and Chen, G.-C. (1994) Polarization-divarison interferometry: far-infrared dichroism. *Appl. Spectrosc.* 48, 1410–1418.
- Polavarapu, P.L. and Deng, Z.Y. (1996) Measurement of vibrational circular dichroism below similar to 600cm⁻¹: progress towards meeting the challenge. *Appl. Spectrosc.* 50, 686–692.

- Ramian, G. (1992) The new UCSB free-electron lasers. *Nucl. Instrum. Methods Phys. Res.* A318, 225–229.
- Ren, L., Martin, C.H., Wise, K.J., Gillespie, N.B., Luecke, H., Lanyi, J.K., Spudich, J.L., and Birge, R.R. (2001) Molecular mechanism of spectral tuning in sensory rhodopsin II. *Biochemistry* 40, 13906–13914.
- Sagan, C., Thompson, W.R., Carlson, R., Gurnett, D., and Hord, C. (1993) A search for life on Earth from the Galileo spacecraft. *Nature* 365, 715–721.
- Schellma, J.A. (1973) Vibrational optical activity. *J. Chem. Phys.* 58, 2882–2886.
- Sprecher, C.A. and Johnson, W.C. (1977) Circular dichroism of nucleic-acid monomers. *Biopolymers* 16, 2243–2264.
- Stasiak, A. and Maddocks, J.H. (2000) Best packing in proteins and DNA. *Nature* 406, 251–253.
- Stuart, J.A. and Birge, R.R. (1996) Characterization of the primary photochemical events in bacteriorhodopsin and rhodopsin. In *Biomembranes, Vol. 2A*, edited by A.G. Lee, JAI Press, London, pp. 33–140.
- Tama, F. and Brooks, C.L. (2002) The mechanism and pathway of pH induced swelling in cowpea chlorotic mottle virus. *J. Mol. Biol.* 318, 733–747.
- Tama, F., Gadea, F.X., Marques, O., and Sanejouand, Y.H. (2000) Building-block approach for determining low-frequency normal modes of macromolecules. *Proteins* 41, 1–7.
- Thomas-Keppta, K.L., Bazylinski, D.A., Kirschvink, J.L., Clemett, S.J., McKay, D.S., Wentworth, S.J., Vali, H., Gibson E.K., Jr., and Romanek, C.S. (2000) Elongated prismatic magnetite crystals in ALH84001 carbonate globules: potential Martian magnetofossils. *Geochim. Cosmochim. Acta* 64, 4049–4081.
- van Vlijmen, H.W.T. and Karplus, M. (1999) Analysis of calculated normal modes of a set of native and partially unfolded proteins. *J. Phys. Chem. B* 103, 3009–3021.
- Wang, W.Q. and Liang, Z. (2001) From parity to chirality—experimental search for parity-violating energy difference of alanine and valine enantiomers. *Acta Physico-Chim. Sinica* 17, 1077–1085.
- Williams, B.S., Callebaut, H., Kumar, S., Hu, Q., and Reno, J.L. (2003) 3.4-THz quantum cascade laser based on longitudinal-optical-phonon scattering for depopulation. *Appl. Phys. Lett.* 82, 1015–1017.
- Woolard, D.L., Globus, T.R., Gelmont, B.L., Bykhovskaia, M., Samuels, A.C., Cookmeyer, D., Hesler, J.L., Crowe, T.W., Jensen, J.O., Jensen, J.L., and Loerop, W.R. (2002) Submillimeter-wave phonon modes in DNA macromolecules. *Phys. Rev. E* 65, 051903/1–11.
- Yee, D.P., Chan, H.S., Havel, T.F., and Dill, K.A. (1994) Does compactness induce secondary structure in proteins—a study of poly-alanine chains computed by distance geometry. *J. Mol. Biol.* 241, 557–573.
- Zolotov, M. and Shock, E. (1999) Abiotic synthesis of polycyclic aromatic hydrocarbons on Mars. *J. Geophys. Res. Planets* 104, 14033–14049.

Address reprint requests to:

Dr. Kevin W. Plaxco

Department of Chemistry and Biochemistry
University of California, Santa Barbara
Santa Barbara, CA 93106

E-mail: kwp@chem.ucsb.edu

Dr. S. James Allen

Department of Physics
University of California, Santa Barbara
Santa Barbara, CA 93106

E-mail: allen@quest.ucsb.edu

Dr. Robert R. Birge

Department of Chemistry
The University of Connecticut
Storrs, CT 06269

E-mail: rbirge@uconn.edu